Advance Publication

Circulation Journal
doi:10.1253/circj.CJ-24-0254

ORIGINAL ARTICLE

Role of Optical Coherence Tomography in Vasculitis-Associated Pulmonary Hypertension and Chronic Thromboembolic Pulmonary Hypertension

Burçak Kilickiran Avci, MD; Emire Seyahi, MD; Fuat Polat, MD; Zeynep Kolak, RA; Hakan Yalman, MD; Ersan Atahan, MD; Hurrem Gul Ongen, MD; Zeki Ongen, MD

Background: Identifying and understanding the microstructural changes within the wall of the pulmonary artery (PA) is crucial for elucidating disease mechanisms and guiding treatment strategies. We assessed the utility of optical coherence tomography (OCT) in identifying such changes within segmental/subsegmental PAs and compared the morphological variations in WHO group 4 pulmonary hypertension associated with Behcet Disease (BD), Takayasu arteritis (TA) and chronic thromboembolic pulmonary hypertension (CTEPH). Idiopathic pulmonary arterial hypertension (IPAH) patients served as controls.

Methods and Results: A total of 197 cross-sectional images were analyzed from 20 consecutive patients. BD patients exhibited lower %wall area and mean wall thickness (MWT) compared with CTEPH, TA and, IPAH patients. TA patients showed a notably higher %wall area, which was significant in IPAH and BD patients. Variations in %wall area measurements were observed across distinct cross-sectional segments of the PA within individual patients (22% in CTEPH, 19% in BD, 16% in TA, 23% in IPAH patients). Intravascular webs, bands, and thrombi were observed in BD and CTEPH patients. OCT provided clear delineation of vascular wall calcifications and adventitial vasa vasorum. No procedure-related complications were observed.

Conclusions: PA involvement differs among the various etiologies of PH, with the PA being heterogeneously affected. OCT offers promise in elucidating microstructural vascular wall changes and providing insights into disease mechanisms and treatment effects.

Key Words: Behcet disease; Chronic thromboembolic pulmonary hypertension; Idiopathic pulmonary arterial hypertension; Optical coherence tomography; Takayasu arteritis

Detailed in vivo characterization of the wall of the pulmonary artery (PA) assists in understanding the effect of distinct disease etiologies on the pulmonary vasculature. Optical coherence tomography (OCT) has emerged as a valuable technique of intravascular imaging, renowned for its high resolution (10–20 μm). It is primarily used for qualitative and quantitative analyses of atherosclerotic coronary plaque properties, enabling the distinction of individual plaque types such as fibrous, lipid-rich, and calcified plaques, as well as the quantitation of lipid content and macrophage burden, and vasa vasorum (VV) enlargement.[1–7] In the pulmonary vasculature, OCT has been mainly employed to demonstrate vascular wall thickness in patients with idiopathic pulmonary arterial hypertension (IPAH) or scleroderma-associated PAH, and for VV evaluation in children with congenital heart disease.[8–15] Additionally, OCT has proven valuable in assessing intraluminal lesions, such as web, bands, and stenosis, in chronic thromboembolic pulmonary hypertension (CTEPH).[16,17] However, its role in evaluating the vascular wall properties of the distal PA in distinct etiologies in group-4 PH remains underexplored, warranting further studies.

Group 4 PH primarily results from PA obstruction by blood clots,[18,19] and it is essential to recognize other etiologies that contribute to PA obstruction, with vasculitis emerging as a significant contributor that may sometimes be misdiagnosed as CTEPH.

Behcet disease (BD) and Takayasu arteritis (TA) are notable examples of vasculitic conditions capable of inducing chronic PA obstruction, ultimately leading to group-4 PH.[18–20] BD is a variable vessel vasculitis with systemic implications, occasionally extending to the PA, giving rise to aneurysms or thrombosis within the PA.[21–24] Notably, in BD, the prevailing perspective is that PA occlusion results primarily from in-situ thrombosis rather than embolic

Received April 3, 2024; revised manuscript received May 2, 2024; accepted May 13, 2024; J-STAGE Advance Publication released online June 28, 2024 Time for primary review: 19 days

Department of Cardiology (B.K.A., F.P., Z.K., H.Y., Z.O.), Department of Rheumatology (E.S.), Department of Pulmonary Medicine (E.A., H.G.O.), Cerrahpasa Faculty of Medicine, Istanbul University Cerrahpasa, Istanbul, Turkey

Mailing address: Associate Professor Burcak Kilickiran Avci, MD, Department of Cardiology, Cerrahpasa Faculty of Medicine, Istanbul University-Cerrahpasa, Istanbul, Turkey. email: b.kilickiranavci@iuc.edu.tr

All rights are reserved to the Japanese Circulation Society. For permissions, please email: cj@j-circ.or.jp

ISSN-1346-9843

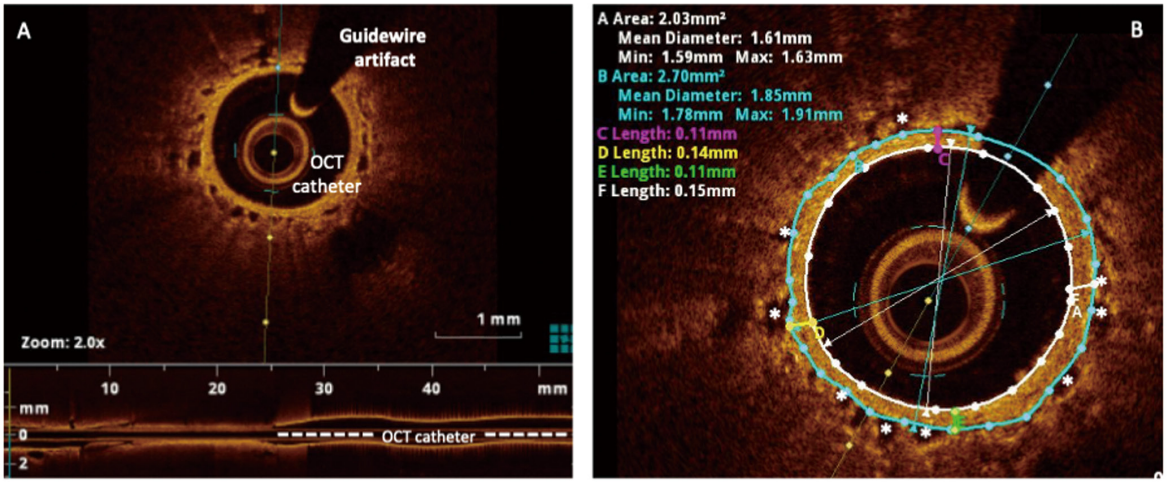


Figure 1. (**A**) Optical coherence tomography (OCT) image displaying a 25-mm longitudinal axis view (**Bottom**) and the most distal cross-sectional image of the visualized subsegmental pulmonary artery (**Top**). (**B**) OCT measurements: white tracing represents the inner lumen area, the blue tracing represents the total vessel area, and measurements on the vascular wall (pink, yellow, green, and white: C,D,E, and F, respectively) indicate measured wall thickness from 4 quadrants. (*) indicate adventitial vasa vasorum.

events, distinguishing it from conventional CTEPH.[21–25] In contrast, TA is a chronic granulomatous pan-arteritis that can affect the PA system, causing stenosis or aneurysmal dilatation.[24,26–30] However, the precise establishment of thrombus formation and a direct cause-effect relationship of thrombus to PA occlusion in TA remains elusive. Current understanding of the underlying pathophysiology of PA involvement and the development of PH in BD and TA is limited and relies primarily on surgical specimens or autopsy findings.

The main goal of this study was to assess the capability of OCT in revealing microstructural changes in the segmental/subsegmental PA. We investigated and compared morphological variations in the pulmonary vasculature in BD-associated PH, TA-associated PH, and CTEPH using OCT. Patients diagnosed with IPAH were included as a control group, enabling a comprehensive analysis of alterations in distal vascular wall characteristics in response to elevated pulmonary pressure.

Methods

Patients

This was a single-center, prospective observational study. Consecutive patients diagnosed with BD with pulmonary involvement, pulmonary vasculitis due to TA, CTEPH or IPAH, who had been referred to the catheterization laboratory for the diagnostic work-up or follow-up right heart catheterization (RHC) for PH, were screened. Patients with severe lung conditions (forced vital capacity <60% or severe pulmonary fibrosis on computed tomography) or left heart disease (severe aortic or mitral valvular heart disease, low left ventricular ejection fraction (<50%)), intracardiac mass or thrombus in the right heart chambers, history of previous pulmonary endarterectomy, occlusion of the superior and inferior vena cava, estimated glomerular filtration rate <60 mL/min, pregnancy, or a history of allergy to contrast media were excluded. Each patient underwent a comprehensive evaluation by a rheumatologist (E.S.). The diagnosis of BD and TA were established according to current guidelines.[31,32] Only patients who had been in remission for ≥1 year were included in the study. PA involvement was based on findings on SPECT-perfusion scan and CTPA or invasive pulmonary angiography that indicated stenosis or occlusion of PA branches. Eligible patients underwent RHC. Patients with a mean PA pressure (mPAP) >20 mmHg with PA wedge pressure (PAWP) or left ventricular end-diastolic pressure (LVEDP) ≤15 mmHg were consecutively enrolled, and OCT was performed at the same session. As an exception, in patients with TA, the PAWP ≤15 mmHg criterion was not applied due to common coexistence of left ventricular diastolic dysfunction in this disease due to systemic hypertension.

The study protocol was approved by the Human Research Ethics Committee of the Cerrahpasa Faculty of Medicine (approval number: 83045809-604.01.02). All procedures adhered to the principles outlined in the Declaration of Helsinki and followed the ethical standards set by the institution's responsible committee on human experimentation. All participants provided written informed consent.

Right Heart Catheterization

RHC was performed with the patient in a supine position without sedation via the femoral vein using a 6F multipurpose or 7F Swan-Ganz catheter. The following hemodynamic parameters were measured: mean right atrial pressure; systolic, diastolic, and mean PAPs; PAWP and/or LVEDP; and systemic arterial pressures. Cardiac output, cardiac index (CI), and pulmonary vascular resistance (PVR) were obtained from the indirect Fick method and assumed basal oxygen consumption.

OCT Imaging

Following the standard RHC procedure, eligible patients

Advance Publication

Table 1. Characteristics of the Patients

	All patients (n=20)	CTEPH (C) (n=7)	BD-PH (B) (n=5)	TD-PH (T) (n=3)	IPAH (I) (n=5)	P value
Sex (M/F)	9/11	3/4	4/1	1/2	1/4	NS
Age, mean±SD, years	49±14	62±10	42±5	43±21	41±8	<0.001[a]
Hypertension n (%)	5 (25)	3 (42.9)	0 (0)	2 (66.7)	0 (0)	0.028
Diabetes, n (%)	2 (10)	1 (14.3)	1 (5)	0 (0)	0 (0)	NS
Smoking, n (%)	1 (5)	0 (0)	1 (20)	0 (0)	0 (0)	NS
CAD, n (%)	2 (10)	1 (14.3)	0 (0)	1 (33.3)	0 (0)	NS
Laboratory values						
Pro-BNP, pg/mL	462±608	752±823	89±78	283±320	536±578	<0.001[b]
Creatinine, mg/dL	0.79±0.24	0.93±0.27	0.86±0.17	0.62±0.03	0.61±0.17	NS
Hemoglobin, g/dL	12.7±1.5	12.8±1.5	13.7±0.83	11.5±0.53	12.2±2.0	NS
Drugs n (%)						
ERA	4 (20)	1 (14.3)	1 (20)	0 (0)	2 (40)	NS
PDE5I	7 (35)	1 (14.3)	1 (20)	0 (0)	5 (100)	NS
Riociguat	3 (15)	2 (28.6)	1 (20)	0 (0)	0 (0)	NS
Iloprost inhaler	1 (5)	0 (0)	0 (0)	0 (0)	1 (20)	NS
Glucocorticoid	8 (40)	0 (0)	5 (100)	3 (100)	0 (0)	NS
Immunosuppressant	8 (40)	0 (0)	5 (100)	3 (100)	0 (0)	NS

[a]C vs. B, P<0.001; C vs. T, P<0.001; C vs. I, P<0.001. [b]C vs. T, P<0.001; C vs. B, P<0.001; I vs. B, P<0.001. BD, Behcet disease; CAD, coronary artery disease; CTEPH, chronic thromboembolic pulmonary hypertension; ERA, endothelin receptor antagonist; F, female; IPAH, idiopathic pulmonary artery hypertension; M, male; NS, not significant; PDE5I, Phosphodiesterase-5 inhibitor; PH, pulmonary hypertension; TA, Takayasu arteritis.

received 60 U/kg of heparin sodium. To acquire OCT images, a commercially available C7-XR™ imaging system (St. Jude Medical, Inc.) with a LightLab 200 cm Cardiovascular Imaging Wire (LightLab Imaging Inc. UK) was used. The OCT imaging wire was advanced distally into a selected segmental PA with the aim of reaching as far as possible within the targeted PA using a 6F JR4 or MP guiding catheter. After successful delivery of the OCT wire, 70/30 contrast saline mixture was administered by automated injection (with a flow rate of 5 mL/s, infusion time of 4 s, and pressure of 400 psi) to fill the distal vessel during motorized pullback. Images were acquired at a consistent pullback speed of 10 mm/s. If feasible and anatomically accessible, we attempted to image at least 3 different segmental/subsegmental PA per lung. All acquired images were later reviewed offline using dedicated St. Jude Software (The AptiVue™). All OCT measurements were done by the same study investigator (BKA). Only high-quality images without artifacts were used for measurements.

In evaluating vessel lumen characteristics across the patient groups, we carefully examined for the presence of web lesions, band lesions, and thrombus formation. The following measurements were performed in the proximal and distal parts of each visualized segment with clearly imaged wall borders: lumen diameter, wall thickness, inner lumen area, and total vessel area (**Figure 1**). To evaluate the entire vessel wall comprehensively while accounting for variations in vessel size, we calculated the wall area and %wall area. Wall thickness measurements from each quadrant of the PA were obtained, and clearly defined maximal wall thickness (MWT) was used for subsequent comparisons. The mean vessel lumen diameter and inner lumen area were automatically calculated using software. The total vessel area was manually traced, and the wall area was determined by subtracting the inner lumen area from the total vessel area. The %wall area was calculated as (wall area/total vessel area)×100.

As reported in previous studies,[8,9] the PA wall is generally depicted as a homogeneous, signal-rich single band, making it challenging to distinguish between PA media from the intima. Therefore, we used adventitial VV as a distinguishing feature between the medial and adventitial layers of the vessel (**Figure 1B**). Consequently, vascular wall measurements encompassed the combined intimal and medial layers of the PA wall.

The total duration of the OCT procedure, together with its limitations and associated complications, was recorded. Procedure-related complications encompassed death, bleeding, PA perforation, and embolic events.

Statistical Analysis

Statistical analysis was performed using IBM SPSS version 29.0. P<0.05 was considered statistically significant. Continuous variables are summarized as mean±standard deviation (SD), and categorical variables are presented as absolute values and percentages. Group comparisons were made using one-way ANOVA analysis, followed by Bonferroni or Duncan's multiple comparison tests as appropriate. The relationships between variables were assessed using Pearson's or Spearman's correlation coefficient. To evaluate intra-observer variability, the same cardiologist (BKA) conducted measurements on the same 10 randomly selected cross-sectional vessel images, following a 2-month interval from the last patient enrollment. Interobserver variability was assessed by a second investigator (Z.O.) who was unaware of the previous results and performed measurements on 10 randomly selected segments. Intraclass correlation coefficients (ICCs) were calculated to assess the agreement in measurements of PA maximum wall thickness, lumen diameter, lumen area, and total vessel area both within and between observers.

Table 2. Right Heart Catheterization and OCT Findings

	All patients	CTEPH (C)	BD-PH (B)	TA-PH (T)	IPAH (I)	P value
Total meas.*	197	74	43	33	47	
Total meas./pp	9.9±2.1	10.6±2.2	8.6±1.9	10.3±2.5	9.8±0.9	NS
Heart catheterization						
RAP (mmHg)	8.3±2.8	9.4±2.8	5.7±1.0	9.3±1.0	8.3±3.2	<0.001[a]
sPAP (mmHg)	59.5±25.9	63.8±18.4	39.7±13.4	49.7±12.4	76.0±34.9	<0.001[b]
mPAP (mmHg)	36±14.1	38.3±8.8	26.8±6.6	26.7±3.6	46.3±19.9	<0.001[b]
PAWP (mmHg)	12.1±3.0	12.9±2.9	10±1.9	15.5±1.7	10.3±1.8	<0.001[c]
PVR (WU)	5.6±5.3	5.2±2.7	2.5±1.2	2.8±0.6	10.5±7.9	<0.001[d]
CI (L/min/m^2)	2.7±0.8	2.6±0.8	3.0±0.8	3.2±0.9	2.4±0.5	<0.001[e]
Optical coherence tomography						
Lumen diam. (mm)	3.5±1.0	3.5±1.0	3.7±0.9	3.1±0.8	3.4±1.2	0.034[f]
Lumen area (mm^2)	10.1±5.7	10.1±5.7	11.4±5.0	7.9±4.4	10.3±6.7	NS
Wall area (mm^2)	2.5±1.3	2.6±1.1	2.3±1.4	2.5±1.4	2.5±1.4	NS
%wall area	21.1±7.0	21.5±5.5	17.3±4.8	25.2±9.3	21.1±7.3	<0.001[g]
MWT (mm/100)	25.6±9.2	26.5±6.1	21.5±8.2	29.5±11.7	25.6±10.8	0.002[h]

*Total number of measured cross-sections. Total meas./pp, total measured cross-sections per patient. Apart from the total measurement value, all values are expressed as mean ± SD. [a]I vs. B, P: 0.002; C vs. B, P<0.001; T vs. B, P<0.001. [b]I vs. T, P<0.001; I vs. B, P<0.001; C vs. T, P<0.001; C vs. B, P<0.001. [c]I vs. C, P<0.001; I vs. T, P<0.001; C vs. T, P<0.001; C vs. B, P<0.001: T vs. B, P<0.001. [d]I vs. C, P: 0.010; I vs. T, P<0.001; I vs. B, P<0.001; C vs. T, P: 0.029; C vs. B, P: 0.005. [e]I vs. T, P<0.001; I vs. B, P<0.001; C vs. T, P<0.001; C vs. B, P: 0.006. [f]T vs. B, P: 0.020. [g]I vs. T, P: 0.043; I vs. B, P: 0.041; C vs. T, P: 0.063; C vs. B, P: 0.006; T vs. B, P<0.001. [h]C vs. B, P: 0.021; T vs. B, P: 0.001, I vs. B, P: 0.155. CI, cardiac index; mPAP, mean pulmonary artery pressure; MWT, maximal wall thickness; NS, not significant; PAWP, pulmonary arterial wedge pressure; PVR, pulmonary vascular resistance; RAP, right atrial pressure; segm., segment; sPAP, systolic pulmonary artery pressure.

Results

Clinical Characteristics

Between May 2019 and May 2022, 43 patients were initially screened and 20 were excluded from undergoing OCT imaging for the following reasons: left heart disease (n=3), severe lung conditions (n=2), right ventricular thrombus (n=1), chronic occlusion of superior and inferior vena cava (n=1), previous endarterectomy history (n=3), chronic kidney disease (n=2), mPAP <20 mmHg on RHC (n=4) or unwillingness to participate in the study (n=4). Ultimately, the study included 5 patients with BD-associated PH, 5 with TA-associated PH, 8 with CTEPH and 5 with IPAH for OCT examination. One patient initially diagnosed with CTEPH was excluded from final analysis due to severe lung disease and 2 patients with TA were excluded due to poor OCT image quality.

Table 1 and **Table 2** provide an overview of the clinical characteristics and hemodynamic variables of the patients, respectively. The mean age of the patients was 49±14 years, ranging from 29 to 73 years. Notably, none of the patients with BD and IPAH exhibited systemic hypertension, in contrast to 2/3 patients with TA and 3/7 patients with CTEPH (P=0.028). Additionally, CTEPH patients were older than those in the other groups (P<0.001).

Patients with IPAH and CTEPH exhibited elevated levels of pro-B-type natriuretic peptide, PVR, and mPAP compared with those with BD and TA. Significant differences in RHC measurements were observed among the study groups (**Table 2**). sPAP, mPAP, and PVR were significantly higher in patients with IPAH and CTEPH than in those with BD and TA. Additionally, RAP was significantly lower in BD compared with the other groups. PAWP was significantly increased in patients with CTEPH and TA compared with IPAH and BD. Additionally, the CI in the IPAH and CTEPH groups was significantly lower than in the BD and TA groups.

OCT Imaging and Measurements

We analyzed a total of 108 pullbacks, with an average of 5.4±1.1 segmental vessels per patient, which resulted in a total of 197 cross-sectional measurements taken from the segmental-subsegmental PAs. The entire OCT procedure ranged in duration from a minimum of 26 min to a maximum of 95 min, with a mean duration of 53±19.8 min following placement of the guiding catheter in the desired location within the PA. The mean contrast dosage used during the procedure was 130.6±15.6 mL. A detailed comparison of OCT findings among the 4 groups is presented in **Table 2**.

Figure 2 illustrates cross-sectional image samples for all 4 groups. Overall, the MWT appeared thinner within the BD group, demonstrating significant differences when compared with CTEPH and TA (P=0.021 and P=0.001, respectively), while showing nonsignificant differences with IPAH (P=0.155). Notable variations in wall thickness were observed across all quadrants in a cross-section, particularly in TA patients. Maximum difference in wall thickness in the same cross-section was 0.066 mm in TA, 0.031 mm in BD, 0.030 mm in IPAH, and 0.018 mm in CTEPH. This quadrant-specific variation underscores the potential value of %wall area measurements, which account for all quadrants and are proportional to the total vessel area, providing more consistent information about wall thickening. The %wall area measurements revealed significant thickening of the vascular wall in the TA group compared with the other groups. Statistical significance was primarily observed compared with BD and IPAH (P≤0.001 and P=0.043, respectively), with nonsignificant differences noted with CTEPH (P=0.063). Conversely, the BD group showed lower %wall area compared with the other groups (P=0.006 for CTEPH, P≤0.001 for TA, and P=0.041 for

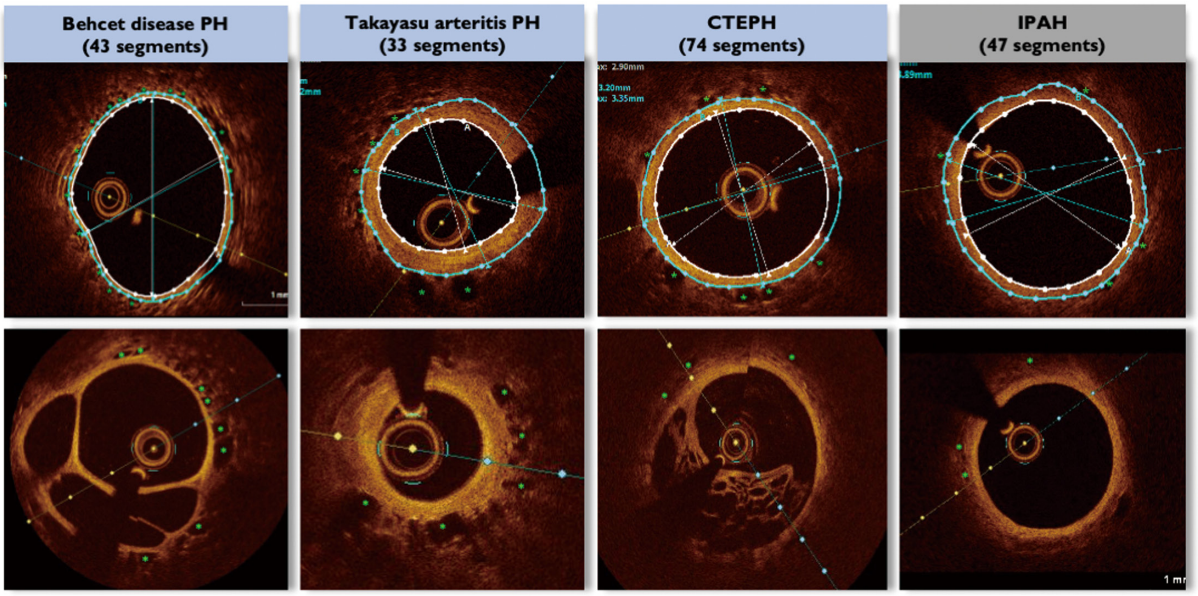


Figure 2. Representative Optical coherence tomography (OCT) images for each disease group and control (IPAH). (**Upper**) Cross-sectional vessel wall area. (**Lower**, **Left** to **Right**) Intraluminal web lesion in a patient with Behcet disease; thickened vascular wall and enlarged vasa vasorum in a patient with Takayasu arteritis; mesh lesion in a patient with CTEPH. There is also a stitch artifact at the 12 o'clock position. (*) Adventitial vasa vasorum microvessels that vary in shape and volume in each image.

Table 3. Correlations Between %Wall Area and MWT With Hemodynamic Parameters

Group	Cor. Coef. Significance	sPAP	mPAP	PVR
%wall area				
CTEPH	r	0.380	0.314	0.061
	P	<0.001	0.062	0.608
Behcet – PH	r	–0.193	0.026	–0.386
	P	0.222	0.917	0.011
Takayasu – PH	r	–0.168	–0.391	–0.173
	P	0.366	0.167	0.352
IPAH	r	0.532	0.656	0.363
	P	<0.001	<0.001	0.010
MWT				
CTEPH	r	0.271	0.273	–0.024
	P	0.019	0.103	0.103
Behcet – PH	r	0.097	0.488	–0.045
	P	0.530	0.025	0.770
Takayasu – PH	r	–0.401	–0.511	0.141
	P	0.028	0.062	0.458
IPAH	r	0.626	0.701	0.397
	P	<0.001	<0.001	0.004

Abbreviations as in Tables 1,2.

IPAH).

Another notable finding was the considerable heterogeneity in %wall area measurements across distinct cross-sectional segments of the PA within individual patients. Notably, the maximum change in %wall area attained 23% and 22% for IPAH and CTEPH, respectively. In the case of BD, this variation was 19% and 16% for TA. These findings underscored the intrinsic diversity in wall thickening of the PA vasculature even within the same patient, highlighting the heterogeneity of the disease process.

The ICCs demonstrated excellent agreement for both inter- and intra-observer analyses in mean diameter, lumen area, and total vascular area measurements (all >0.9). The MWT parameter exhibited good agreement in both intra-

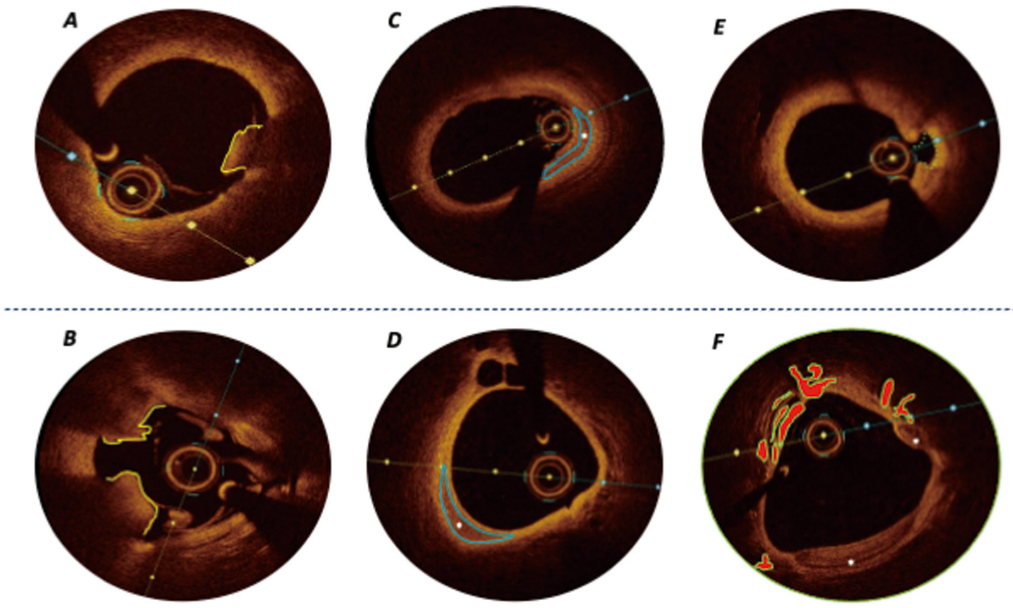


Figure 3. (**A**,**B**) Yellow tracings represent wall-adherent thrombus in patients with BD and CTEPH, respectively. (**C**,**D**) Blue tracings represent calcification in the vascular wall of patients with CTEPH. (**E**) Green tracing represents vasa vasorum (VV) directly connected with the pulmonary artery lumen. (**F**) Green and red represent external and internal VV, respectively. (*) Calcification. BD, Behcet disease; CTEPH, chronic thromboembolic pulmonary hypertension.

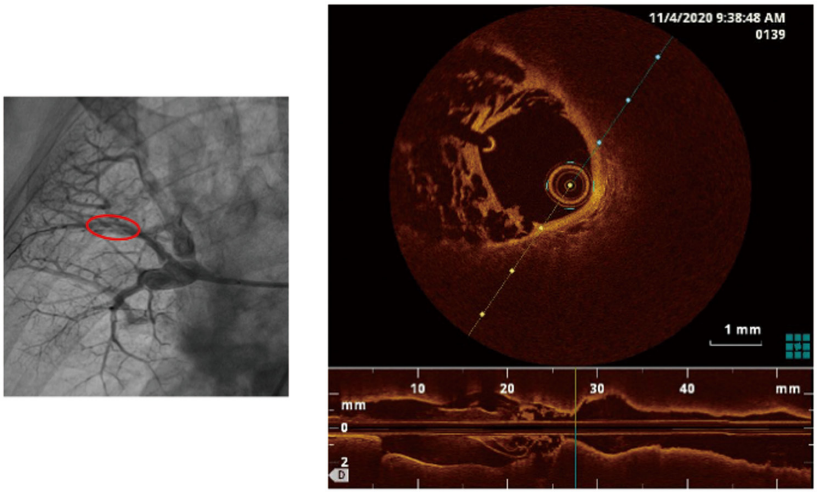


Figure 4. Pulmonary angiogram and corresponding optical coherence tomography image of the investigated upper lobe segmental pulmonary artery. The red circle on the pulmonary angiogram indicates the matching area of the cross-sectional and longitudinal OCT images, which shows an intraluminal mesh lesion.

and interobserver measurements, with coefficients of 0.755 and 0.723, respectively.

OCT Findings

Pulmonary Hemodynamics We found a high positive correlation between wall area and lumen area across all patients (r=0.721, P<0.001). However, there was only a weak positive correlation between mean vessel lumen diameter and MWT (r=0.296, P<0.001).

Among patients with IPAH, a moderate positive correlation was observed between %wall area and MWT measured by OCT, and pulmonary hemodynamic parameters (mPAP and sPAP) (**Table 3**). Conversely, in the CTEPH group, only sPAP exhibited fair correlation with %wall area and MWT. Within the BD group, a moderate correlation was found solely between MWT and mPAP. In contrast, no positive correlations were found between any hemodynamic parameter and wall measurements in patients with TA. PVR showed modest positive correlations with %wall area and MWT in the IPAH group exclusively.

Intravascular Morphology OCT showed intravascular

Advance Publication

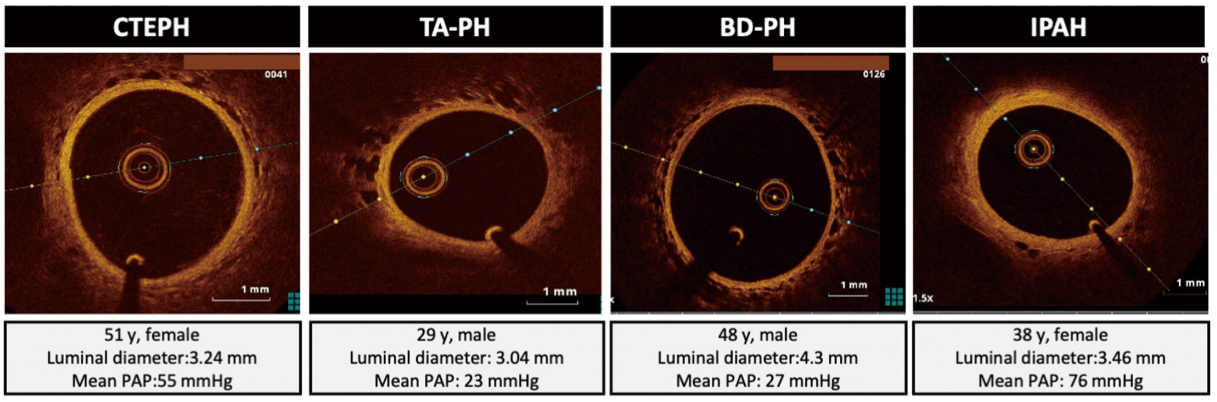


Figure 5. Varying size and number of adventitial vasa vasorum observed in the cross-sectional images of the pulmonary artery affected by different disease etiologies. Vasa vasorum are observed as lacunae beyond the signal-rich intima-media layer. BD, Behcet disease; CTEPH, chronic thromboembolic pulmonary hypertension (PH); IPAH, idiopathic pulmonary arterial hypertension; TA, Takayasu arteritis.

lesions, including webs, bands, and thrombus with notably high image quality, surpassing that of invasive angiography and CT pulmonary angiography (**Figures 3**,**4**). Both CTEPH and BD-PH patients exhibited these lesions, characterized by similar morphologies. In contrast, no obstructive fibrotic lesions were observed in the investigated segmental/subsegmental branches among patients in the IPAH and TA-PH groups.

Observational Findings at the Vascular Wall Adventitial VV were visualized, displaying greater volume especially in TA-PH, and increased in number in individuals with BD-PH and CTEPH (**Figures 1**,**2**,**5**) as compared with those with IPAH. Additionally, vascular wall calcification was observed in specific cross-sectional images of patients with CTEPH and TA (**Figure 3**).

Limitations of OCT

The diameter of the distal end of the OCT catheter is 1 mm and the minimum lumen diameter we could image was 1.3 mm. Although we could visualize vessels with a luminal diameter of up to 6 mm in some segments, the overall image quality was unsatisfactory in vessels >5 mm because of poor resolution issues. Another technical challenge involved obtaining clear images from tortuous PAs, which proved particularly problematic in the TA group.

Complications After OCT

No procedure-related complications were observed, but 2 thrombotic events occurred after the OCT procedure. Neither of these complications was directly attributed to OCT itself. In 1 case, a patient with CTEPH experienced acute intracardiac thrombus formation approximately 24 h after the procedure, potentially related to anticoagulation interruption and hematoma development in the femoral area. In another instance, a patient with BD presented with deep vein thrombosis approximately 2 days post- procedure, with this event presumed to be related to BD activation.

Discussion

Determining the PA involvement characteristics in diverse etiologies leading to occlusion in the pulmonary vasculature and PH is crucial for understanding the features of the disease and guiding therapy. Advanced microstructural assessment, beyond conventional imaging, is needed, with OCT emerging as a promising tool.[8,9] However, investigations into PA wall remodeling with OCT have been limited in number. Specifically, only 1 study has examined this aspect in patients with CTEPH,[13] and 1 study has explored it in pulmonary TA-PH,[33] but none has focused on patients with pulmonary BD-associated PH. This study is the first attempt to use OCT to evaluate and compare vascular remodeling in PH patients with PA obstruction attributed to BD, TA, or CTEPH.

Our findings revealed that OCT can provide significant information regarding the extent of pulmonary vascular remodeling in the segmental and subsegmental PA across diverse clinical scenarios. PA wall thickness increased in all patient groups, compared with historical controls reported as 0.162 mm in an autopsy series and 0.13 and 0.19 mm, respectively in in-vivo studies.[8,12,13] Because vascular wall thickness was not uniform in cross-sectional images in the 4 quadrants of the artery in the current study, we used %wall area as the main parameter to represent wall thickening. Consequently, the pulmonary vascular wall was significantly thicker in the TA group and conversely, the vascular wall in BD-PH tended to be thinner than in other groups.

The thickening of the PA wall in IPAH was mainly attributed to increased pulmonary pressure. Consistent with the study by Dai et al,[12] we found a significant correlation between wall thickness and mPAP in IPAH patients. However, in CTEPH and BD, the correlation between pulmonary pressure and wall thickness appeared weak. In TA pulmonary pressure did not seem to be the primary contributor to increased vascular wall thickness. Although we could not definitively conclude the effect of severe elevation of PAP on thickening of the PA wall due to the limited number of patients with slightly elevated PAP, it can be speculated that disease-related inflammation plays a pivotal role in wall thickness in TA and BD.

CTEPH and BD-PH are considered distinct clinical enti-

ties, but our investigation revealed notable parallels in their intraluminal characteristics. Regardless of the primary pathogenic mechanism, whether stemming from embolism or in-situ thrombosis, both conditions manifested conspicuous similarities in the presence of chronic thrombi with irregular intimal structures or recanalized formations, leading to fibrous webs and bands spanning the vascular lumen. These shared intraluminal features prompt consideration of the potential utility of pulmonary endarterectomy in BD-PH, particularly given its efficacy in CTEPH.[34] However, caution is essential, especially in active BD, as surgical intervention may elevate the risk of thrombosis. Additionally, operative risk and postoperative disease progression should be taken into consideration.[34]

Conversely, the imaging of segmental/subsegmental vessels in TA-PH and IPAH did not reveal comparable intraluminal thrombotic patterns. Yanagisawa et al included 4 patients with pulmonary TA-PH in their study in which they identified the presence of intraluminal thrombus within the lesions.[33] However, the primary focus of their study was to establish therapeutic efficacy and the underlying mechanisms of percutaneous pulmonary angioplasty for treating peripheral pulmonary stenosis and pulmonary TA-PH using OCT. Their study did not provide information regarding the types of thrombotic lesions (i.e., recanalized lesions like band, web, or mesh lesions) and the underlying thrombotic mechanisms. In contrast, Gong et al reported in-situ thrombosis, particularly in the proximal PA in TA, which differs from the recanalized thrombus formations observed in CTEPH or BD.[35] These differences suggest variations in the development and healing processes of thrombi in TA, where thrombus formation may not be the predominant contributor to distal vessel obstruction.

VV form a microvascular network on the wall of arteries to supply nutrients and oxygen to the wall. VV enrichment on histology has been demonstrated in systemic arterial walls and has been explained as mainly related to inflammation in vasculitis.[36] Within the PA wall, VVs contribute to vascular integrity, and emerging evidence emphasizes a more prominent role for the adventitial layer and VVs in PH development.[37] An increase in the volume of pulmonary adventitial VV has been described in pathological specimens obtained from patients with CTEPH and IPAH, and expansion of the VV may participate in pathologic pathways.[38,39] Nevertheless, studies investigating the PA microvasculature using OCT remain limited.[14,15] Examining the images from our study, adventitial VV in the PA wall appeared enlarged, especially in TA, increased in number in BD and CTEPH and with relatively less enrichment in IPAH. However, due to the lack of appropriate software for calculating VV density, definitive conclusions regarding the relationship between disease or hemodynamic parameters and these VV changes remain elusive. Some cross-sections in the CTEPH and TA groups displayed evidence of vascular wall calcification, possibly indicating the chronic nature of the disease.

Our data demonstrate that %wall area and intraluminal findings and the distribution of VVs were not uniform throughout the evaluated PA segments. Therefore, assessment of a single PA segment may not represent the underlying disease state. Multi-segmental imaging by OCT may provide a complete picture of pulmonary vascular remodeling and may have an advantage over histopathological examinations using a single tissue sample.

Imaging the vascular network in vivo may aid in understanding disease progression and detecting inflammatory activity within the arterial wall, potentially guiding the development of new therapies for PH by revealing changes in vascular wall properties. Additionally, it may help distinguish patients with active vasculitis from those with quiescent vasculitis. However, further studies are needed to validate these assumptions.

Study Limitations

Limitations of our study include the small, heterogeneous study population and technical challenges. The rarity of diseases such as BD and TA, especially when they involve the PA and lead to PH, coupled with the absence of established exclusion criteria, posed a significant challenge in assembling a large study cohort. It would be important to acknowledge that the limited sample size may affect the generalizability of our findings. Nonetheless, we evaluated as many segments as possible. Our study provides valuable insights into this under-investigated area and should be viewed as a pilot study. Due to ethical concerns, healthy control groups were not included.

Technical limitations of OCT include its time-consuming nature when used for the extensive coverage of the pulmonary segmental and subsegmental arteries, challenges in visualizing wider vessels, and limitations in tortuous vascular anatomy affecting catheter manipulation and image quality. Furthermore, measurement-related limitations include inaccurate delineation of the adventitial border, potentially leading to overestimation of wall thickness and area.

Careful anticoagulation management is essential during and after the procedure, particularly in Group 4 PH patients. Due to the heightened risk of thrombotic complications in BD patients, assessing for active inflammation and initiating appropriate immunosuppressive therapy before interventions is advisable.

Conclusions

OCT is a valuable technique for assessing microstructural changes in the segmental and subsegmental PA wall in vivo. In addition to evaluating intraluminal lesions and vascular wall thickness, OCT can potentially visualize the microvascular network and vascular calcification. This pilot study has demonstrated that vascular remodeling in the distal PA may vary among patients with BD-PH, TA-PH, CTEPH, and IPAH. In addition, vascular remodeling was found to be heterogenous throughout the pulmonary vasculature in these conditions, highlighting the need for comprehensive evaluation. Another important observation was that increased vascular wall thickness in patients with group 4 PH was not primarily attributable to elevated pulmonary pressure. Further studies are crucial to establish OCT's reliability in assessing disease-related changes and response to therapy.

Acknowledgments

This work was supported by funds from ADHAD (Pulmonary Vascular Research Association in Turkey, a non-profit organization).

Conflict of Interest

We declare that none of the authors have any conflicts of interest related to this research. No author was employed by or consulted for any companies in the medical industry involved in this study.

Advance Publication

IRB Information

The study protocol was approved by the Human Research Ethics Committee of the Cerrahpasa Faculty of Medicine (3 April 2018, A-50, document number: 83045809-604.01.02).

Data Availability

The deidentified participant data will be shared on a request basis. Please directly contact the corresponding author to request data sharing.

References

1. Yabushita H, Bouma BE, Houser SL, Aretz HT, Jang IK, Schlendorf KH, et al. Characterization of human atherosclerosis by optical coherence tomography. *Circulation* 2002; **106:** 1640–1645.
2. Kume T, Akasaka T, Kawamoto T, Watanabe N, Toyota E, Neishi Y, et al. Assessment of coronary intima–media thickness by optical coherence tomography: Comparison with intravascular ultrasound. *Circ J* 2005; **69:** 903–907.
3. Montarello NJ, Nelson AJ, Verjans J, Nicholls SJ, Psaltis PJ. The role of intracoronary imaging in translational research. *Cardiovasc Diagn Ther* 2020; **10:** 1480–1507.
4. Fujii K, Kubo T, Otake H, Nakazawa G, Sonoda S, Hibi K, et al. Expert consensus statement for quantitative measurement and morphological assessment of optical coherence tomography: Update 2022. *Cardiovasc Interv Ther* 2022; **37:** 248–254.
5. Sibbald M, Pinilla-Echeverri N, Alameer M, Chavarria J, Dutra G, Sheth T. Using Optical coherence tomography to identify lipid and its impact on interventions and clinical events. A scoping review. *Circ J* 2021; **85:** 2053–2062.
6. Choi BJ, Matsuo Y, Aoki T, Kwon TG, Prasad A, Gulati R, et al. Coronary endothelial dysfunction is associated with inflammation and vasa vasorum proliferation in patients with early atherosclerosis. *Arterioscler Thromb Vasc Biol* 2014; **34:** 2473–2477.
7. Park KH, Kwon TG, Matsuzawa Y, Sun T, Liu Z, Lennon RJ, et al. Association between the vasa vasorum and the atherosclerotic changes in cardiac allograft vasculopathy: Volumetric analysis. *Eur Heart J Cardiovasc Imaging* 2016; **17:** 272–279.
8. Li N, Zhang S, Hou J, Jang IK, Yu B. Assessment of pulmonary artery morphology by optical coherence tomography. *Heart Lung Circ* 2012; **21:** 778–781.
9. Jorge E, Baptista R, Calisto J, Faria H, Monteiro P, Pan M, et al. Optical coherence tomography of the pulmonary arteries: A systematic review. *Int J Cardiol* 2016; **67:** 6–14.
10. Domingo E, Grignola JC, Aguliar R, Montero MA, Arredondo C, Vazquez M, et al. In vivo assessment of pulmonary arterial wall fibrosis by intravascular optical coherence tomography in pulmonary arterial hypertension: A new prognostic marker of adverse clinical follow-up. *Open Respir Med J* 2013; **7:** 26–32.
11. Schwaigner JP, Loder CD, Dobarro D, Kaier T, Reddecliffe S, Schreiber BE, et al. Optical coherence tomography evaluation of pulmonary arterial vasculopathy in systemic sclerosis. *Sci Rep* 2017; **7:** 43304.
12. Dai Z, Fukumoto Y, Tatebe S, Sugimura K, Miura Y, Nochioka K, et al. OCT imaging for the management of pulmonary hypertension. *JACC Cardiovasc Imaging* 2014; **7:** 843–845.
13. Jiang X, Peng FH, Liu QQ, Zhao QH, He J, Jiang R, et al. Optical coherence tomography for hypertensive pulmonary vasculature. *Int J Cardiol* 2016; **222:** 494–498.
14. Hayabuchi Y, Homma Y, Kagami S. Three-dimensional imaging of pulmonary arterial vasa vasorum using optical coherence tomography in patients after bidirectional Glenn and Fontan procedures. *Eur Heart J Cardiovasc Imaging* 2021; **22:** 941–949.
15. Hayabuchi Y, Homma Y, Kagami S. Optical Coherence Tomography for observing development of pulmonary arterial vasa vasorum after bidirectioanl cavopulmonary connection in children. *PLoS One* 2019; **14:** e0215146.
16. Ishiguro H, Kataoka M, Inami T, Shimura N, Yanagisawa R, Kawakami T, et al. Diversity of lesion morphology in CTEPH analyzed by OCT, pressure wire, and angiography. *JACC Cardiovasc Imaging* 2016; **9:** 324–325.
17. Hong C, Luo F, Liu C, Zhong N, Lİ J, Wang W. Clinical study of optical coherence tomography in the diagnosis of peripheral pulmonary artery thrombus. *Thromb Res* 2018; **161:** 52–59.
18. Galie N, Humbert M, Vachiery JL, Gibbs S, Lang I, Torbicki A, et al. 2015 ESC/ERS Guidelines for the diagnosis and treatment of pulmonary hypertension. *Eur Heart J* 2016; **37:** 67–119.
19. Humbert M, Kovacs G, Hoeper MM, Badagliacca R, Berger RMF, Brida M, et al. 2022 ESC/ERS Guidelines for the diagnosis and treatment of pulmonary hypertension. *Eur Heart J* 2022; **43:** 3618–3731.
20. Frost A, Badesch D, Gibbs SR, Gopolan D, Khanna D, Manes A, et al. Diagnosis of pulmonary hypertension. *Eur Respir J* 2019; **53:** 1801904.
21. Seyahi E, Melikoglu M, Akman C, Hanuryudan V, Ozer H, Hatemi G, et al. Pulmonary artery involvement and associated lung disease in Behçet disease: A series of 47 patients. *Medicine (Baltimore)* 2012; **91:** 35–48.
22. Springer J, Villa-Forte A. Thrombosis in vasculitis. *Curr Opin Rheumatol* 2013; **25:** 19–25.
23. Seyahi E, Yazici H. Behçet's syndrome: Pulmonary vascular disease. *Curr Opin Rheumatol* 2015; **27:** 18–23.
24. Adams TN, Zhang D, Batra K, Fitzgerald JE. Pulmonary manifestations of large, medium, and variable vessel vasculitis. *Respir Med* 2018; **145:** 182–191.
25. Yamashita Y, Morimoto T, Kimura T. Venous thromboembolism: Recent advancement and future perspective. *J Cardiol* 2022; **79:** 79–89.
26. Arita Y, Ishibashi T, Nakaoka Y. Current immunosuppressive treatment for Takayasu arteritis. *Circ J* 2023, doi:10.1253/circj.CJ-23-0780.
27. Seyahi E. Takayasu arteritis: An update. *Curr Opin Rheumatol* 2017; **29:** 51–56.
28. He Y, Lv N, Dang A, Cheng N. Pulmonary artery involvement in patients with Takayasu arteritis. *J Rheumatol* 2020; **47:** 264–272.
29. Kerr KM, Auger WR, Fedulla PF, Channik RH, Yi ES, Moser KM. Large vessel pulmonary arteritis mimicking chronic thromboembolic disease. *Am J Resp Crit Care Med* 1995; **152:** 367–373.
30. Kong X, Ma L, Lv P, Cui X, Chen R, Ji Z, et al. Involvement of the pulmonary arteries in patients with Takayasu arteritis: A prospective study from a single centre in China. *Arthritis Res Ther* 2020; **22:** 131.
31. International Team for the Revision of the International Criteria for Behcet's Disease (ITR-ICBD). The International Criteria for Behcet's Disease (ICBD): A collaborative study of 27 countries on the sensitivity and specificity of the new criteria. *J Eur Acad Dermatol Venereol* 2014; **28:** 338–347.
32. Arend WP, Michel BA, Bloch DA, Hunder GG, Calabrese LH, Edworthy SM, et al. The American College of Rheumatology 1990 criteria for the classification of Takayasu arteritis. *Arthritis Rheum* 1990; **33:** 1129–1134.
33. Yanagisawa R, Kataoka M, Inami T, Fukuda K, Yoshino H, Satoh T. Intravascular imaging-guided percutaneous transluminal pulmonary angioplasty for peripheral pulmonary stenosis and pulmonary Takayasu arteritis. *J Heart Lung Transplant* 2016; **35:** 537–540.
34. Yildizeli SO, Yanartas M, Tas S, Direskeneli H, Mutlu B, Ceyhan B, et al. Outcomes of patients with Behçet's syndrome after pulmonary endarterectomy. *Thorac Cardiovasc Surg* 2018; **66:** 187–192.
35. Gong J, Yang Y, Ma Z, Guo X, Wang J, Kuang T, et al. Clinical and imaging manifestation of Takayasu arteritis with pulmonary hypertension: A retrospective cohort study in China. *Int J Cardiol* 2019; **276:** 224–229.
36. Kaiser M, Younge B, Bjornsson J, Goronzy JJ, Weyand CM. Formation of new vasa vasorum in vasculitis: Production of angiogenic cytokines by multinucletaed giant cells. *Am J Pathol* 1999; **155:** 765–774.
37. Stenmark KR, Frid MG, Yeager M, Li M, Riddle S, Mckisey T, et al. Targeting the adventitial microenvironment in pulmonary hypertension: A potential approach to therapy that considers epigenetic change. *Pulm Circ* 2012; **2:** 3–14.
38. Mitzner W, Wagner EM. Vascular remodeling in the circulations of the lung. *J Appl Physiol* 2004; **97:** 1999–2004.
39. Montani D, Perros F, Gambaryan N, Girerd B, Dorfmuller P, Price LC, et al. C-Kit-positive cells accumulate in remodeled vessels of idiopathic pulmonary arterial hypertension. *Am J Respir Crit Care Med* 2011; **184:** 116–123.